# Which Prior Knowledge? Quantification of In Vivo Brain $^{13}$C MR Spectra Following $^{13}$C Glucose Infusion Using AMARES

Bernard Lanz,[1,2] João M. N. Duarte,[1,2] Nicolas Kunz,[1,3] Vladimir Mlynárik,[1] Rolf Gruetter,[1,4,5] and Cristina Cudalbu[1]*

The recent developments in high magnetic field $^{13}$C magnetic resonance spectroscopy with improved localization and shimming techniques have led to important gains in sensitivity and spectral resolution of $^{13}$C in vivo spectra in the rodent brain, enabling the separation of several $^{13}$C isotopomers of glutamate and glutamine. In this context, the assumptions used in spectral quantification might have a significant impact on the determination of the $^{13}$C concentrations and the related metabolic fluxes. In this study, the time domain spectral quantification algorithm AMARES (advanced method for accurate, robust and efficient spectral fitting) was applied to $^{13}$C magnetic resonance spectroscopy spectra acquired in the rat brain at 9.4 T, following infusion of [1,6-$^{13}C_2$] glucose. Using both Monte Carlo simulations and in vivo data, the goal of this work was: (1) to validate the quantification of in vivo $^{13}$C isotopomers using AMARES; (2) to assess the impact of the prior knowledge on the quantification of in vivo $^{13}$C isotopomers using AMARES; (3) to compare AMARES and LCModel (linear combination of model spectra) for the quantification of in vivo $^{13}$C spectra. AMARES led to accurate and reliable $^{13}$C spectral quantification similar to those obtained using LCModel, when the frequency shifts, J-coupling constants and phase patterns of the different $^{13}$C isotopomers were included as prior knowledge in the analysis. **Magn Reson Med 69:1512–1522, 2013.** 

**Key words:** $^{13}$C NMR spectroscopy; spectral quantification; brain; AMARES; isotopomer; prior knowledge

## INTRODUCTION

In vivo dynamic $^{13}$C magnetic resonance spectroscopy (MRS) together with the administration of $^{13}$C-enriched substrates is a powerful and unique technique to noninvasively investigate brain metabolites and metabolic fluxes related to enzyme activities in the in vivo brain (1–6). In particular, the measurement of $^{13}$C incorporation into different carbon positions of glutamate and glutamine in conjunction with an appropriate mathematical model of compartmentalized cerebral metabolism (2,4) allowed the quantitative measurement of important pathways involved in energy metabolism including, but not limited to: glycolysis, tricarboxylic acid (TCA) cycle, malate-aspartate shuttle activity and the glial pyruvate carboxylase. In addition, the glutamate-glutamine cycle between neurons and astrocytes can be measured (1–4,7–13). Further separation of the glial and neuronal TCA cycle activities is possible when measuring the C3 and C2 positions of glutamate and glutamine, due to the glial-specific activity of pyruvate carboxylase, diluting the position 3 and labeling the position 2 of glial glutamate (2) when infusing [1,6-$^{13}C_2$] glucose.

The main advantage of $^{13}$C MRS stands mainly in its increased chemical shift dispersion allowing the detection not only of different molecules but also of specific carbon positions within the same molecule (the so-called $^{13}$C isotopomers) (above 150 ppm – carbon atoms in carbonyl groups; 100–60 ppm – carbon atoms in hydroxyl groups; 60–45 ppm – carbon atoms in CH groups; 45–25 ppm – carbon atoms in $CH_2$ groups and below 25 ppm – carbon atoms in $CH_3$ groups). The low sensitivity of in vivo $^{13}$C MRS can be overcome by the use of $^{13}$C-enriched substrates. In animals, widely used $^{13}$C-enriched substrates are [1-$^{13}$C] or [1,6-$^{13}C_2$] glucose. [1,6-$^{13}C_2$] glucose gives a labeling pattern similar to [1-$^{13}$C] glucose, however the fractional enrichment (FE) of pyruvate (and of all subsequent metabolic pools) can be twice as high, thus improving the detection sensitivity. Moreover, the probability of $^{13}$C isotopes in adjacent positions increases (by a factor of four for two adjacent carbon positions) and consequently the splitting of resonances due to homonuclear $^{13}$C-$^{13}$C scalar coupling giving rise to isotopomer resonances becomes more important. Recently, other $^{13}$C-enriched substrates have also been used (i.e., [2-$^{13}$C] glucose, [2-$^{13}$C] acetate) to discriminate glial and neuronal metabolism (3,14,15).

In the past decade, the measurements at high magnetic fields combined with improvements in localization techniques and with excellent shimming have led to important gains in sensitivity and spectral resolution of $^{13}$C in vivo spectra (1,2,13–16). Signals from 18 different resonances can be detected in the in vivo rat brain after infusion of [1,6-$^{13}C_2$] glucose. Among these resonances,

[1]Laboratory for Functional and Metabolic Imaging (LIFMET), Center for Biomedical Imaging (CIBM), Ecole Polytechnique Fédérale de Lausanne (EPFL), Lausanne, Switzerland.

[2]Faculty of Biology and Medicine, University of Lausanne, Lausanne, Switzerland.

[3]Department of Pediatrics, University of Geneva, Geneva, Switzerland.

[4]Department of Radiology, University of Geneva, Geneva, Switzerland.

[5]Department of Radiology, University of Lausanne, Lausanne, Switzerland.

Additional Supporting Information may be found in the online version of this article.

Grant sponsor: SNF; Grant numbers: 131087, 122498; Grant sponsor: EU; Grant number: MRTN-CT-2006-035801; Grant sponsors: Centre d'Imagerie BioMédicale (UNIL, UNIGE, HUG, CHUV, EPFL, Leenaards and Jeantet Foundations).

*Correspondence to: Cristina Cudalbu, Laboratory for Functional and Metabolic Imaging (LIFMET), Center for Biomedical Imaging (CIBM), Ecole Polytechnique Fédérale de Lausanne (EPFL), Station 6 CH F1 602 (Bâtiment CH), CH-1015 Lausanne, Switzerland. E-mail: cristina.cudalbu@epfl.ch

Received 15 March 2012; revised 30 May 2012; accepted 13 June 2012.

DOI 10.1002/mrm.24406

Published online 8 August 2012 in Wiley Online Library (wileyonlinelibrary.com).

the signals of alanine (Ala), lactate (Lac), *N*-acetylaspartate, γ-aminobutyrate, glutamine (Gln), glutamate (Glu), aspartate (Asp), glucose (Glc) labeled at different carbon positions were measured (1,2,9,16,17). Consequently, the amount of information that can be obtained from in vivo $^{13}C$ spectra has considerably increased (i.e., signals from different carbon positions combined with a fine structure arising from $^{13}C$-$^{13}C$ J-couplings) (17).

To quantify $^{13}C$ MRS spectra, methods based on the incorporation of prior knowledge improved quantification, especially in the presence of overlapping signals (17). In a recent study (17) it has been shown that LCModel analysis combined with a simulated basis set of each isotopomer with appropriate chemical shift and J-coupling pattern allows robust and reliable dynamic $^{13}C$ isotopomers analysis in the in vivo rat brain at 9.4T. Thus, LCModel has become popular in quantifying in vivo $^{13}C$ spectra. LCModel has an important number of attractive features, but for the quantification of $^{13}C$ spectra it requires significant adjustments (i.e., of the control file) to adapt the original program to $^{13}C$ data. In addition, it also requires a specific basis set of each isotopomer with appropriate chemical shift and J-coupling pattern. AMARES, an improved interactive time domain method for accurate and efficient parameter estimation of MRS signals with use of prior knowledge (18), represents an alternative approach to LCModel for the quantification of in vivo $^{13}C$ spectra, since in vivo $^{13}C$ spectra are typically characterized by flat baseline and increased chemical shift dispersion. One of the main advantages relies in the fact that no simulated metabolite basis set is needed when quantifying the in vivo spectra. The signals (resonances) to be quantified are manually selected and the prior knowledge is given in terms of relative or fixed amplitudes, frequencies, linewidths, phases and lineshapes. This advantage increases the flexibility for the user, and consequently any error created by the user can additionally lead to unreliable metabolite quantification. Moreover, fitting the signals arising from different carbon positions with singlets and neglecting the multiplets due to $^{13}C$-$^{13}C$ J-couplings might lead to substantial errors in the quantification of the time courses which would consequently lead to errors in the estimated metabolic fluxes. To the best of our knowledge the impact of prior knowledge in AMARES has never been reported for quantification of $^{13}C$ isotopomers in the in vivo rat brain at high magnetic field.

Therefore, the purpose of this study was: (1) to assess the impact of the prior knowledge on the quantification of in vivo $^{13}C$ isotopomers using AMARES combined with low-level to high-level prior knowledge; (2) to validate the quantification of in vivo $^{13}C$ isotopomers using AMARES; and (3) to compare AMARES and LCModel for the quantification of in vivo $^{13}C$ spectra. The impact of the prior knowledge on quantification and the validation of AMARES were performed using Monte Carlo simulations and in vivo quantifications at 9.4T in the rat brain.

## METHODS

### Animals

All experimental procedures involving animals were approved by the local ethics committee. In vivo localized $^{13}C$ spectra were acquired on Sprague-Dawley rats (275 to 325g, $n = 4$) fasted overnight. The rats were intubated and artificially ventilated with 2% isoflurane (Attane, Minrad, NY) during the surgery. The left and right femoral arteries and veins were catheterized for monitoring blood gases, blood pressure, glucose concentration, and for infusion of α-chloralose (Acros Organics, Geel, Belgium) and [1,6-$^{13}C_2$] glucose (Isotec, Sigma-Aldrich, Basel, Switzerland). After preparation, anesthesia was switched from isoflurane to α-chloralose by injecting an initial 80 mg/kg bolus of α-chloralose, followed by continuous infusion at a rate of ~26.7 mg/kg/h (2). The animals were placed in a home-built holder with the head stereotaxically immobilized. Respiration rate and blood pressure were measured throughout the experiment (SA Instruments, NY). Body temperature was measured with a home-built rectal probe and maintained stable at 38°C ± 0.5°C using a heated water circuit. Arterial blood was sampled approximately every 30 min to monitor blood gases (AVL Compact 3, Diamond Diagnostics, MA) and measure plasma glucose (Reflotron Plus analyzer, Roche Diagnostics GmbH, Mannheim, Germany) and lactate (GW7 Micro-Stat, Analox Instruments, London, UK) concentrations.

The glucose infusion protocol was adapted from previous studies (1,2,16) to achieve a fast increase to a stable level of plasma glucose FE (step function). An exponentially decaying bolus of 99%-enriched [1,6-$^{13}C_2$] glucose solution (1.1 M in a saline solution) was administrated over 5 min. The volume of this bolus was adapted to the measured glycemia to achieve a 70% plasma fractional enrichment at the end of the 5 minutes. A continuous infusion of 70%-enriched glucose was further applied for the remaining 6 h. Glucose was infused at a rate adjustable to the concomitantly measured plasma glucose concentrations to maintain the desired glycemia levels (around 300 mg/dL).

### $^{1}H$ and $^{13}C$ MRS

Localized $^{13}C$ spectra were acquired on a Varian Direct Drive (Palo Alto, CA) console interfaced to an actively shielded 9.4T magnet (Magnex Scientific, Oxford, UK) with a 31-cm horizontal bore. The magnet was equipped with 12 cm inner-diameter actively shielded gradient sets giving a maximum gradient of 400 mT/m in 120 μs. Acquisitions were done using: a home-built 10 mm ($^{13}C$)/13 mm ($^{1}H$ quad) surface coil as radiofrequency transceiver. The rat brain was positioned in the isocenter of the magnet and fast-spin-echo images (repetition time = 4 s, echo time = 52 ms, slice thickness of 1 mm and an in plane resolution of 94 μm) were acquired to determine anatomical landmarks and further position the volume of interest, consisting of a 320 μL voxel (5 × 8 × 8 $mm^3$) in the brain. The static field homogeneity was adjusted using first- and second-order shims with FASTMAP (19,20). To measure the total concentration of the metabolites of interest, $^{1}H$ MRS spectra were acquired before starting glucose infusion using the SPECIAL sequence (21) (repetition time = 4 s, echo time = 2.8 ms, 160 averages, 5 × 8 × 8 $mm^3$). The $^{13}C$ MRS dynamic acquisition was performed in the same voxel (320 μL) with a temporal resolution of 5.4 min, using the semiadiabatic

Table 1
Details on the High-Level Prior Knowledge Used in AMARES for the Quantifications with the 2nd and 3rd Approach

| Resonance | Multiplet | Frequency | Relative phase | Amplitude |
|---|---|---|---|---|
| GlnC3 | GlnC3S | 27.15–27.25 ppm | 0.0 | Estimated |
| | GlnC3D-1 | GlnC3S–18.45 Hz | 34.6 | Estimated |
| | GlnC3D-2 | GlnC3S+16.45 Hz | −34.6 | GlnC3D-1*1.0 |
| | GlnC3T-1 | GlnC3S+32.9 Hz | −69.1 | GlnC3T-2*0.5 |
| | GlnC3T-2 | GlnC3S–2 Hz | 0.0 | Estimated |
| | GlnC3T-3 | GlnC3S–36.9 Hz | 69.1 | GlnC3T-2*0.5 |
| GluC3 | GluC3S | 27.8–27.9 ppm | 0.0 | Estimated |
| | GluC3D-1 | GluC3S+16.3 Hz | −34.3 | Estimated |
| | GluC3D-2 | GluC3S–18.3 Hz | 34.2 | GluC3D-1*1.0 |
| | GluC3T-1 | GluC3S–2 Hz | 0.0 | Estimated |
| | GluC3T-2 | GluC3S+32.6 Hz | −68.5 | GluC3T-1*0.5 |
| | GluC3T-3 | GluC3S–36.6 Hz | 68.5 | GluC3T-1*0.5 |
| GlnC4 | GlnC4S | 31.74–31.84 ppm | 0.0 | Estimated |
| | GlnC4D43-1 | GlnC4S–18.45 Hz | 34.6 | Estimated |
| | GlnC4D43-2 | GlnC4S+16.45 Hz | −34.6 | GlnC4D43-1*1.0 |
| GluC4 | GluC4S | 34.3–34.4 ppm | 0.0 | Estimated |
| | GluC4D43-1 | GluC4S+16.3 Hz | −34.3 | Estimated |
| | GluC4D43-2 | GluC4S+18.3 Hz | 34.3 | GluC4D43-1*1.0 |
| GlnC2 | GlnC2S | 55.15–55.25 ppm | 0.0 | Estimated |
| | GlnC2D23-1 | GlnC2S+17.45 Hz | −34.6 | Estimated |
| | GlnC2D23-2 | GlnC2S–17.45 Hz | 34.6 | GlnC2D23-1*1.0 |
| | GlnC2D21-1 | GlnC2S+25.7 Hz | 0.0 | Estimated |
| | GlnC2D21-2 | GlnC2S–27.7 Hz | 0.0 | GlnC2D21-1*1.0 |
| GluC2 | GluC2S | 55.65–55.75 ppm | 0.0 | Estimated |
| | GluC2D23-1 | GluC2S+16.3 Hz | −34.3 | Estimated |
| | GluC2D23-2 | GluC2S-18.3 Hz | 34.3 | GluC2D23-1*1.0 |
| | GluC2D21-1 | GluC2S+25.7 Hz | 0.0 | Estimated |
| | GluC2D21-2 | GluC2S–27.7 Hz | 0.0 | GluC2D21-1*1.0 |

distortionless enhancement by polarization transfer (DEPT) technique (repetition time = 2.5 s, interpulse delay 3.8 ms ($J_{CH}$= 130 Hz), 45° for last $^{1}$H pulse to simultaneously measure signals from CH, $CH_2$, $CH_3$ groups) (16). Localization was performed using 3D-ISIS (image selected in vivo spectroscopy) (hyperbolic secant inversion pulses (22), 2 ms duration, 8 kHz bandwidth) combined with outer volume suppression (23).

## Data Analysis

In vivo $^{13}$C spectra were quantified using four approaches (1st, 2nd, and 3rd approach based on AMARES (18) and 4th approach based on LCModel (24,25) used as a "gold standard" for validation purposes). In this study, we fitted only the isotopomers of Glu C4, C3, C2 and of Gln C4, C3, C2 since their time courses are the principal ones used for metabolic modeling. Henry et al. (17) showed that accurate quantification of aspartate can be obtained at 9.4T with a temporal resolution of 22 min, whereas 1 h accumulation was necessary for γ-aminobutyrate. Increasing the magnetic field to 14.1T allowed quantification of aspartate with a temporal resolution of 5.3 min, as shown by Duarte et al. (2), but the estimated fluxes did not change significantly with the inclusion of aspartate turnover curves.

1. 1st approach: AMARES with low-level prior knowledge: each resonance at a specific carbon position (Glu C4, C3, C2 and Gln C4, C3, C2) was fitted using a singlet without any information on the J-coupling pattern (for example, the multiplets of Glu at the position 4 were fitted using only one singlet). The following constraints were used: relative phases (fixed to zero) and Lorentzian lineshape. No constraints were given on the amplitudes, linewidths or frequencies.
2. 2nd approach: AMARES combined with medium-level prior knowledge, identical with that used by LCModel (isotopomers with the same chemical shift and J-coupling pattern, see Table 1) with the exception that the information on the relative phases (due to homonuclear $^{13}$C-$^{13}$C *J*-modulation occurring during the delay between the $^{13}$C excitation and acquisition in the DEPT sequence) was neglected, i.e., the relative phases was fixed to zero. Each isotopomer was fitted using lorentzian lines with the following constraints:
   - linewidths: the linewidth of the GluC4 singlet was estimated, whereas for the other isotopomers we considered identical linewidths to that of the GluC4 singlet.
   - amplitudes: for the singlets the amplitudes were estimated, whereas for the doublets or triplets prior knowledge was given as following: the doublets peaks were considered as having equal amplitudes by using the "fixed ratio" option, and for the triplets we considered the relative intensities of 1:2:1 using the same option.
   - frequencies: soft constraints were given to all the singlets (±0.05 Hz) and the *J* couplings were included using the singlets as reference and the "fixed shift" option.

   More details regarding the prior knowledge can be found in the Table 1.

3. 3rd approach: AMARES combined with high-level prior knowledge, identical with that used by LCModel and by our 2nd approach (isotopomers with the same chemical shift and J-coupling pattern, see Table 1) with additional constraints on relative phases.
   - relative phases: the effect of homonuclear $^{13}C$-$^{13}C$ *J*-evolution during the DEPT sequence was taken into account as described previously (17). The relative phases were calculated for each multiplet. For a triplet the relative phases were calculated as $\theta_0$:0:$-\theta_0$, with $\theta_0 = 2\pi^*\tau^*J_{CC}$ radians. The relative phases for doublet were $\theta_0$:$-\theta_0$, with $\theta_0 = \pi^*\tau^*J_{CC}$ radians. The delay $\tau$ was fixed empirically as previously determined (17).

   The AMARES files containing the prior knowledge used for the 3rd approach are provided as Supporting Information.
4. 4th approach: LCModel combined with a basis set generated using Matlab by simulating each isotopomer with the appropriate chemical shift and J-coupling pattern, as previously described by Ref. 17. The lineshapes were Lorentzian with a linewidth of 4 Hz.

Notations: for consistency similar notations as those used by Refs. 17 and 26 were used in this study. For example, for the glutamate at the position C4 we used GluC4S to designate the singlet and GluC4D43-1 and GluC4D43-2 represent the two lines of the doublet. Overall, a specific multiplet was named using the abbreviation of the metabolite (i.e., Glu for glutamate), followed by the labeled position (i.e., C4 – to indicate the labeling at the carbon position 4) and the specific multiplet structure (i.e., S-singlet, D-doublet, with D43 representing the doublet corresponding to the coupling to the C3, T-triplet and DD-doublet of doublet). As for the previous studies (17) no numbers were added when the coupling constants were identical (i.e., GluC3D is the sum of GluC3D32 and GluC3D34). In addition, GluC4 refers to the sum of all glutamate isotopomers labeled at the position C4.

Some isotopomers were excluded from this study since their probability of being labeled was very low: GluC4D45—doublet of GluC4 corresponding to the coupling between the positions 4 and 5; GluC4DD—doublet of doublet for GluC4 corresponding to the coupling between the positions 3, 4, and 5; GluC2DD—doublet of doublet for GluC2 corresponding to the coupling between the positions 1, 2, and 3; GlnC2DD—doublet of doublet for GlnC2 corresponding to the coupling between the positions 1, 2, and 3. The criteria for excluding these isotopomers was based on the fact that when infusing [1,6-$^{13}C_2$] glucose the positions 1 and 5 are not sufficiently labeled to give a detectable signal in vivo within 5 min of time resolution and consequently their inclusion as prior knowledge would increase the number of parameters to estimate and therefore the incertitude of the quantification. In addition, these isotopomers were neither fitted when using LCModel.

## Brain Metabolism of [1,6-$^{13}C_2$] Glucose

After transport across the blood brain barrier, glucose is metabolized to pyruvate through the glycolysis (27). In the case of [1,6-$^{13}C_2$] glucose, two molecules of [3-$^{13}C$] pyruvate are generated from one molecule of labeled glucose. Pyruvate is metabolized both in the glial and neuronal TCA cycles. When infusing [1-$^{13}C$] glucose, only one molecule of [3-$^{13}C$] pyruvate is produced, while the second pyruvate molecule generated by the glycolysis is unlabeled.

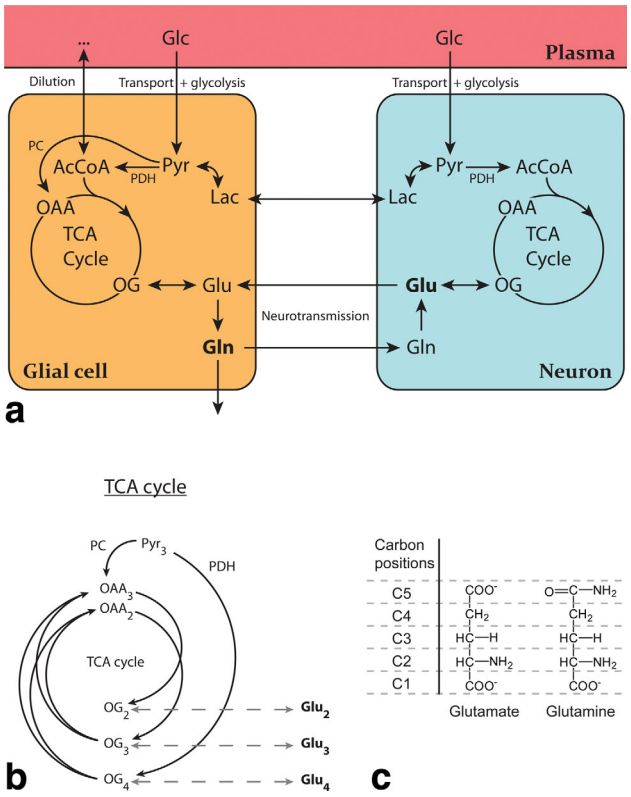


FIG. 1. Description of the $^{13}C$ labeling of glutamate and glutamine through brain metabolic processes. PC: pyruvate carboxylase, PDH: pyruvate dehydrogenase (**a**) two-compartment description of brain glucose metabolism. Glutamate and glutamine are part of the neurotransmission cycle, which interacts both with the neuronal and glial TCA cycles; (**b**) Detail of the transfer of $^{13}C$ to the different carbon positions of glutamate in the TCA cycle. PC is only taking place in the glial TCA cycle. Through the neurotransmission cycle, the glutamine molecules get labeled at the same carbon positions than their respective glutamate precursor; (**c**) Chemical structures of glutamate and glutamine with their corresponding carbon positions. [Color figure can be viewed in the online issue, which is available at wileyonlinelibrary.com.]

Brain metabolism of [1,6-$^{13}C_2$] glucose and the resulting labeling of the carbon positions in the glutamate and glutamine molecules are illustrated in Fig. 1. The $^{13}C$ carbon from [1,6-$^{13}C_2$] glucose reaches the position C4 of 2-oxoglutarate, which exchanges label with the position C4 of cytosolic glutamate trough transmitochondrial exchange. In the second turn of the TCA cycle, through the same exchange process, half of the $^{13}C$ further reaches the position C3 of glutamate and the other half the position C2. In the third turn of the TCA cycle, the position C1 of glutamate gets also labeled, but this position is usually not simultaneously measurable with the positions C4, C3, and C2 using $^{13}C$ MRS, due to the large chemical shift of the C1 carbon signal relative to the other resonances. Some reactions are specific to glial

cells, like pyruvate carboxylase. This reaction brings $^{13}C$ from [3-$^{13}C$] pyruvate to the position 2 of glial glutamate and unlabeled $^{12}C$ to the position 3 of glial glutamate. Additionally, the glial Acetyl-CoA, at the entrance of the TCA cycle, is diluted by alternative energetic fuels that glial cells can metabolize, like acetate and fatty acids (28,29).

The neurotransmission cycle, or glutamate-glutamine cycle, brings $^{13}C$ from glial glutamate to glutamine and further to neuronal glutamate, which labels again glial glutamate. No labeling exchange between the different carbon positions takes place in this cycle, as opposed to the TCA cycles.

The dynamics of labeling of glutamate and glutamine contains information on the glial and neuronal TCA cycles activity and on the neurotransmission cycle (4). The total concentration of $^{13}C$ at a certain carbon position is given by the total intensity of the corresponding $^{13}C$ resonance, independently of its multiplet structure. The percentage of molecules labeled at a certain carbon position, known as fractional enrichment, is directly related to the multiplet pattern of the corresponding resonance (30). Therefore, infusing [1-$^{13}C$] glucose instead of [1,6-$^{13}C_2$] glucose will decrease by a factor 2 the fractional enrichment of each carbon position leading to a decrease by a factor 4 of the doublet intensities and by a factor 8 of the triplet intensities. In the case of [1,6-$^{13}C_2$] glucose infusion, the quantification of the multiplets structure is therefore more critical.

### Monte Carlo Simulations

To estimate the reliability of the estimated concentrations in different experimental conditions, artificial $^{13}C$ MRS spectra representative of brain in vivo spectra obtained at labeling steady-state were simulated with different linewidths and signal to noise ratios (SNRs). The simulated spectra were generated using Matlab (MathWorks, Natick, MA). Each resonance was constructed using previously measured values of the chemical-shift and J-coupling of the different isotopomers measurable in an in vivo spectrum (17) (typically 20 isotopomers of Glu C4, C3, C2 and of Gln C4, C3, C2). For each isotopomer, the corresponding peaks were created by constructing an FID simulated as an oscillating function multiplied by a decaying real exponential function to generate a Lorentzian lineshape with the desired linewidth, frequency and phase, determined as described in Table 1 and in the method 2 of the AMARES data analysis. The FID of each isotopomer was further scaled (relatively to the GluC4S singlet) to the corresponding signal intensity measured in a typical in vivo brain $^{13}C$ spectrum. This was done in the following way: using typical brain metabolic fluxes (2) and total brain metabolite concentrations, the fractional enrichment at labeling steady-state (~280 mins) of the different carbon positions of glutamate and glutamine was calculated. From these fractional enrichments, the amplitude of each isotopomer was calculated as the product of the probabilities of having the corresponding carbons of a molecule labeled and the other neighboring carbons of the same molecule unlabeled. For example, the intensity of the isotopomer GluC3D34 was calculated as the product of the FE of the position C3 and the FE of the position C4 of glutamate, multiplied by (1-$FE_{C2}$). In this particular case, since the chemical shift and J-coupling of the isotopomer GluC3D32 are the same as for GluC3D34, both calculated intensities were added to generate the doublet GluC3D, with half of the summed intensity in each of the two resonances of the doublet.

Based on phantom experiments, the relative isotopomer intensities were further corrected to simulate the detection efficiency of the corresponding resonances by the DEPT sequence at the different chemical shifts, when placing the carrier frequency at 41 ppm.

A random normally distributed noise was added to the sum of the FIDs of each isotopomer. The noise level of the simulated spectra was expressed in terms of SNR, calculated as the peak height of the GluC4S singlet (the highest peak present in a $^{13}C$ spectrum following [1,6-$^{13}C_2$] glucose infusion) divided by twice the root mean square noise. The resulting FID was finally Fourier transformed, resulting in an artificial steady-state $^{13}C$ spectrum.

To compare accuracy and precision of the three different spectral quantification approaches using AMARES (1st, 2nd, and 3rd approach) and consequently the impact of prior knowledge, 200 spectra were generated with a SNR of 10 and a linewidth of 5 Hz and fitted using each of the four methods.

In a second step, the effect of the spectral quality on the quantification was analyzed using different values for the SNR and linewidth (i.e., ranging from poor quality data at SNR of 1 or 2 and linewidth of 10 Hz to good quality data at SNR of 10 and linewidth of 5 Hz). The 3rd approach (AMARES combined with high-level prior knowledge) was selected to analyze changes in the precision and accuracy of the spectral quantification of the carbon positions GluC4, C3, and C2 as well as GlnC4, C3, C2, when decreasing SNR or increasing linewidth. Monte Carlo simulations (based on 200 artificial spectra) were undertaken with a varying SNR of 1, 2, 3, and 10 and a linewidth of 5 Hz. The effect of the linewidth on the quantification was further analyzed with Monte Carlo simulations by increasing linewidth from 5 to 10 Hz, both in the case of a SNR of 3 and 10. Finally, the spectra at SNRs of 1 and 2 and linewidths of 5 and 10 Hz were used to compare the 1st (low-level prior knowledge) and 3rd (high-level prior knowledge) approaches using AMARES, to evaluate the impact of prior knowledge on processing poor quality data (low SNR and large linewidths) and to assess whether the two approaches give similar results at low SNR.

The mean and standard deviation of the fitted peak intensities obtained over 200 spectra were reported and compared to the true peak intensities used for the generation of the artificial spectra. For each metabolite, the bias (difference between the mean value of the amplitude estimates and the true amplitude) was expressed as a percentage of the true amplitude. A positive bias corresponds to an overestimation of the amplitude compared with the true value, and a negative bias to an underestimation of the amplitude. In addition, the standard deviations were expressed as a percentage of the mean values of the amplitude estimates.

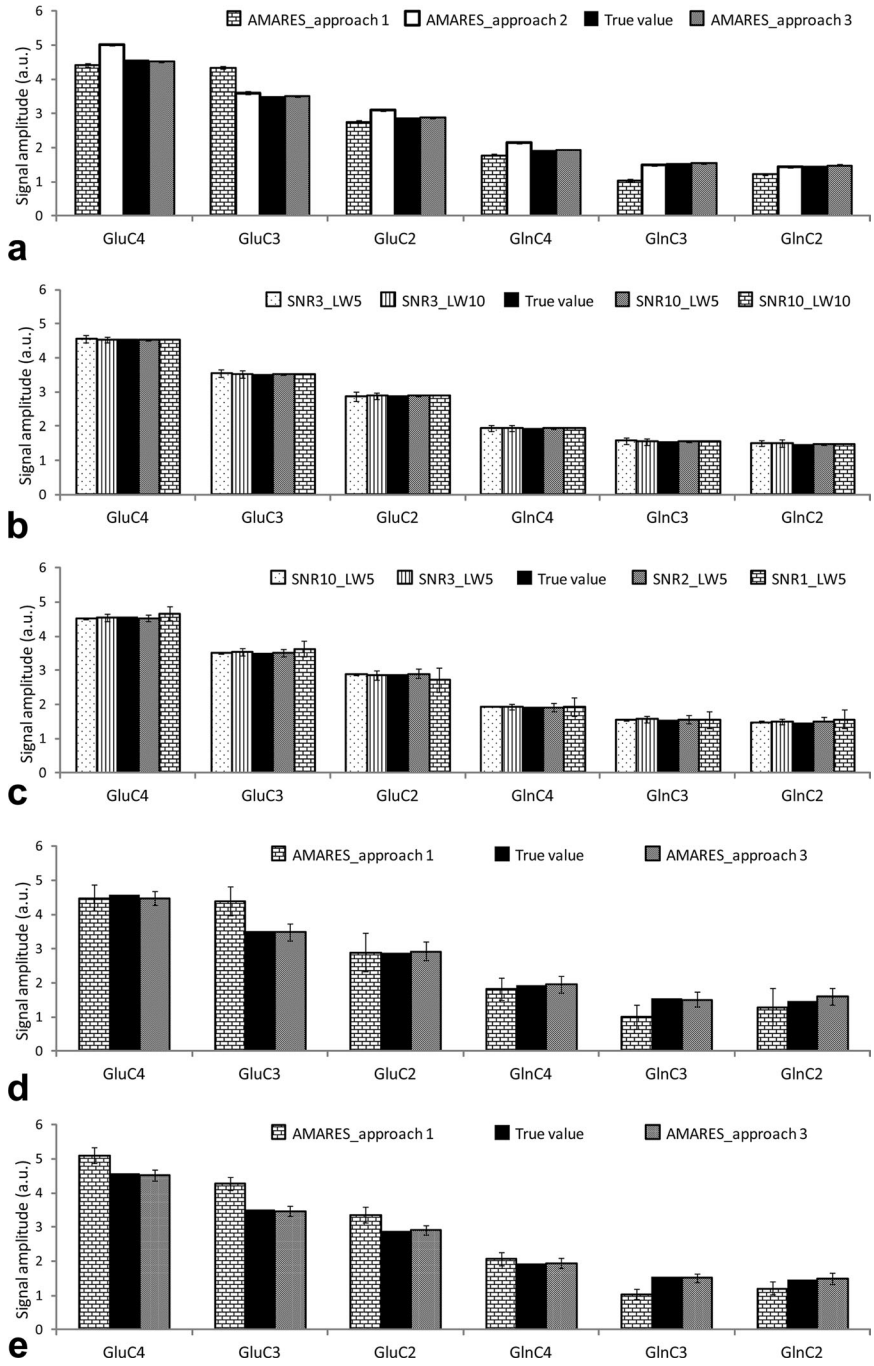


FIG. 2. Effects of increasing prior knowledge in AMARES analyzed with Monte Carlo simulations: (**a**) Quantifications performed using AMARES with the 1st, 2nd, and 3rd approach; (**b**) and (**c**) Quantifications performed using AMARES combined with high-level prior knowledge (3rd approach) for different SNRs and linewidths; (**d**) Quantifications performed using AMARES 1st and 3rd approach on signals with an SNR of 1 and linewidth of 5 Hz; (**e**) Quantifications performed using AMARES 1st and 3rd approach on signals with an SNR of 2 and linewidth of 10 Hz.

## RESULTS

First, Monte Carlo simulations were performed to assess the influence of prior knowledge by quantifying the simulated Monte Carlo signals with the different approaches using AMARES: from low-level to high-level prior knowledge (1st, 2nd, and 3rd approach). In addition, the reliability and robustness of $^{13}C$ isotopomers quantification using AMARES with high-level prior knowledge (3rd approach) was evaluated using different levels of SNR and linewidth. Finally, the impact of prior knowledge on poor quality data was assessed by comparing the 1st (low-level prior knowledge) and 3rd (high-level prior knowledge) approaches using AMARES at SNRs of 1 and 2.

Figure 2a shows the influence of prior knowledge by quantifying the Monte Carlo signals with the different approaches, from low-level to high-level prior knowledge using AMARES (1st, 2nd, and 3rd approach). As can be seen, when low-level prior knowledge was used, meaning that each resonance at a specific carbon position was fitted using a singlet without any information on the *J*-coupling pattern, higher underestimation were obtained for all metabolites (3–42%) except of GluC3 which was overestimated by 23%. The standard deviations were on the order of 2%, meaning that no important variations were obtained. To further evaluate the impact of the prior knowledge, we slightly improved our prior knowledge by adding each isotopomer with chemical shift and

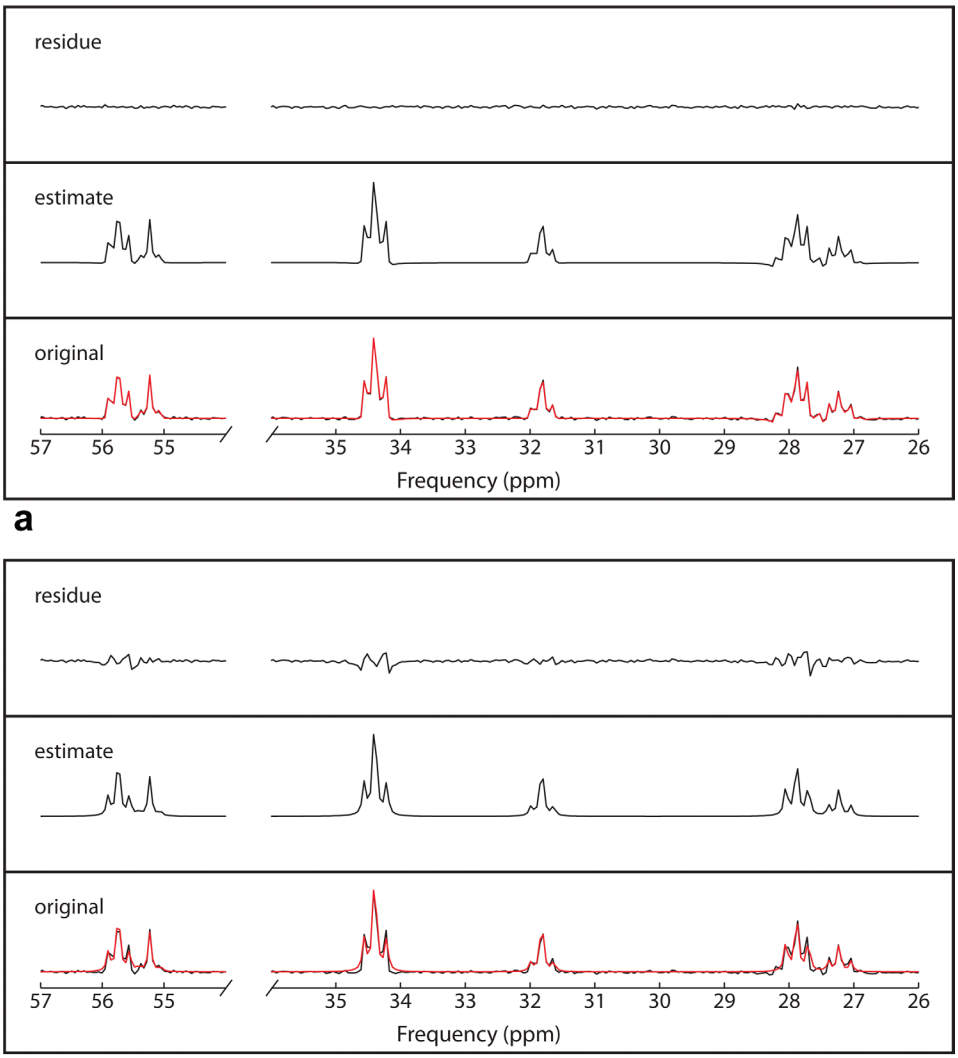


FIG. 3. AMARES quantification of a Monte Carlo signal (SNR of 10, linewidth of 5 Hz) using: (**a**) the high-level prior knowledge (3rd approach) and (**b**) medium-level prior knowledge (2nd approach). From bottom to top: estimate superimposed on the original Monte Carlo signal, estimate and residue. The plotted regions were focused on Glu and Gln C2, C3, and C4 multiplets.

J-coupling information but neglecting the relative phases due to homonuclear $^{13}C$-$^{13}C$ J-modulation occurring during the delay between the $^{13}C$ excitation and acquisition in the DEPT sequence (medium-level prior knowledge, 2nd approach). In this second case the results showed important improvements but slight overestimations ranging from 3 to 11% were still obtained for all the metabolites with the exception of Gln C2 and C3 which were underestimated by 4%. These over/underestimations were also clearly visible in Fig. 3b when looking at the quantification residue. Finally, the 3rd approach with high-level prior knowledge gave consistent and highly similar results to the true values. No under/overestimations were observed and the standard deviations were about 1–2%. The quality of the AMARES fit with high-level prior knowledge was excellent as shown in Fig. 3a.

The reliability and robustness of $^{13}C$ isotopomers quantification using AMARES with high-level prior knowledge (3rd approach) and different levels of SNR and linewidth is shown in Fig. 2b,c. All metabolites were identified using AMARES with high-level prior knowledge (3rd approach), even with small levels of SNR and large linewidths. Overall, for SNRs of 10 and 3 with linewidth between 5 and 10 Hz, the systematic errors were within 2%, well within typical experimental errors. At a very low sensitivity (SNR of 1) the errors increased to 7%. As expected, larger standard deviations (4–16%) were observed with lower SNRs and larger linewidths.

The impact of prior knowledge on poor quality data (SNR of 1 and 2 with linewidth of 5 and 10 Hz) is shown in Fig. 2d,e. All metabolites were correctly identified when using AMARES with high-level prior knowledge (3rd approach) even with the lowest SNR of 1. Systematic errors were within 7% and standard deviations between 4 and 16%. However, when using AMARES with low-level prior knowledge (1st approach), systematic errors increased to 30%.

Figures 4 and 5 show the overall quality of in vivo $^{13}C$ spectra acquired in this study at 9.4T in the rat brain. In vivo spectra contained a considerable amount of information: resonances from glucose C6, glutamate and glutamine C4, C3, C2, aspartate C3, C2 were detected together with smaller resonances from γ-aminobutyrate, *N*-acetylaspartate, aspartate and lactate. The presence of multiple isotopomers was clearly observed in vivo, i.e.,

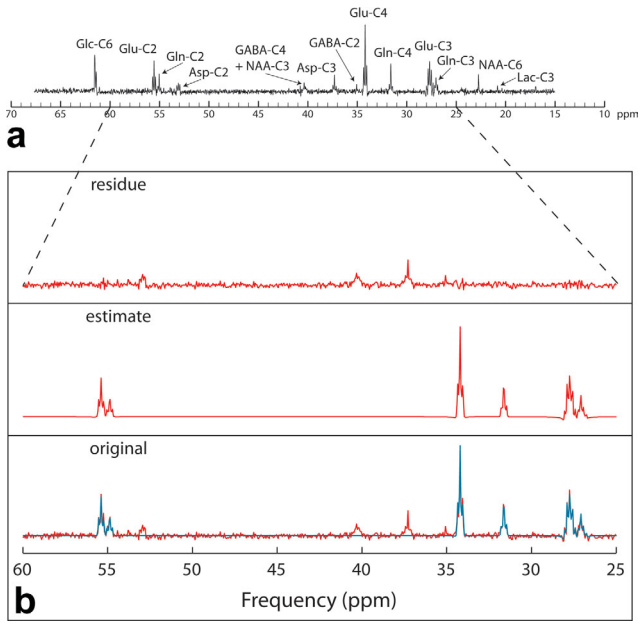


FIG. 4. Quantification of a typical in vivo $^{13}C$ MRS spectrum (**a**) $^{1}H$-localized $^{13}C$ spectrum acquired in vivo on a rat brain after infusion of [1,6-$^{13}C_2$]glucose in a voxel of 320 μL. The data was acquired during 1 h, starting 5 h after the onset of glucose infusion. **b**: AMARES quantification of the signal shown in (a). From bottom to top: estimate superimposed on the original signal, estimate and residue. A zoom was performed on Glu and Gln C3, C4, and C2 multiplets.

the singlet (GluC4S) and doublet resonances (GluC4D43) of GluC4 and the singlet (GluC3S), doublet (GluC3D1, GluC3D2) and triplet (GluC3T1, GluC3T2, GluC3T3, where T1, T2, and T3 represent the three lines of the triplet) resonances for GluC3. The AMARES quantification using high-level prior knowledge (3rd approach) is shown in Fig. 4b. The fit matched the in vivo data as shown by the flat residual. Since the low concentrated metabolites such as γ-aminobutyrate, *N*-acetylaspartate and aspartate were not included in the fit, their resonances were present in the residual.

For the in vivo quantifications, we assessed first the impact of prior knowledge by using AMARES combined with low-level to high-level prior knowledge (i.e., the results obtained using low and medium-level prior knowledge were compared to those obtained using high-level prior knowledge). Figure 5a shows the impact of prior knowledge (AMARES combined with the 1st or 3rd approach) on spectra acquired after 1 hour of [1,6-$^{13}C_2$] glucose infusion (temporal resolution of 5.4 min in a 320 μL voxel). Figure 5b demonstrates the impact of prior knowledge (using AMARES combined with the 1st or 3rd approach) on spectra acquired after 5 h of [1,6-$^{13}C_2$] glucose infusion (temporal resolution of 5.4 min in a 320 μL voxel). As can be seen, the fit matched the in vivo data when using the AMARES quantification with high-level prior knowledge (3rd approach) for both spectra acquired at different time points during the infusion. However, when using the low-level prior knowledge (1st

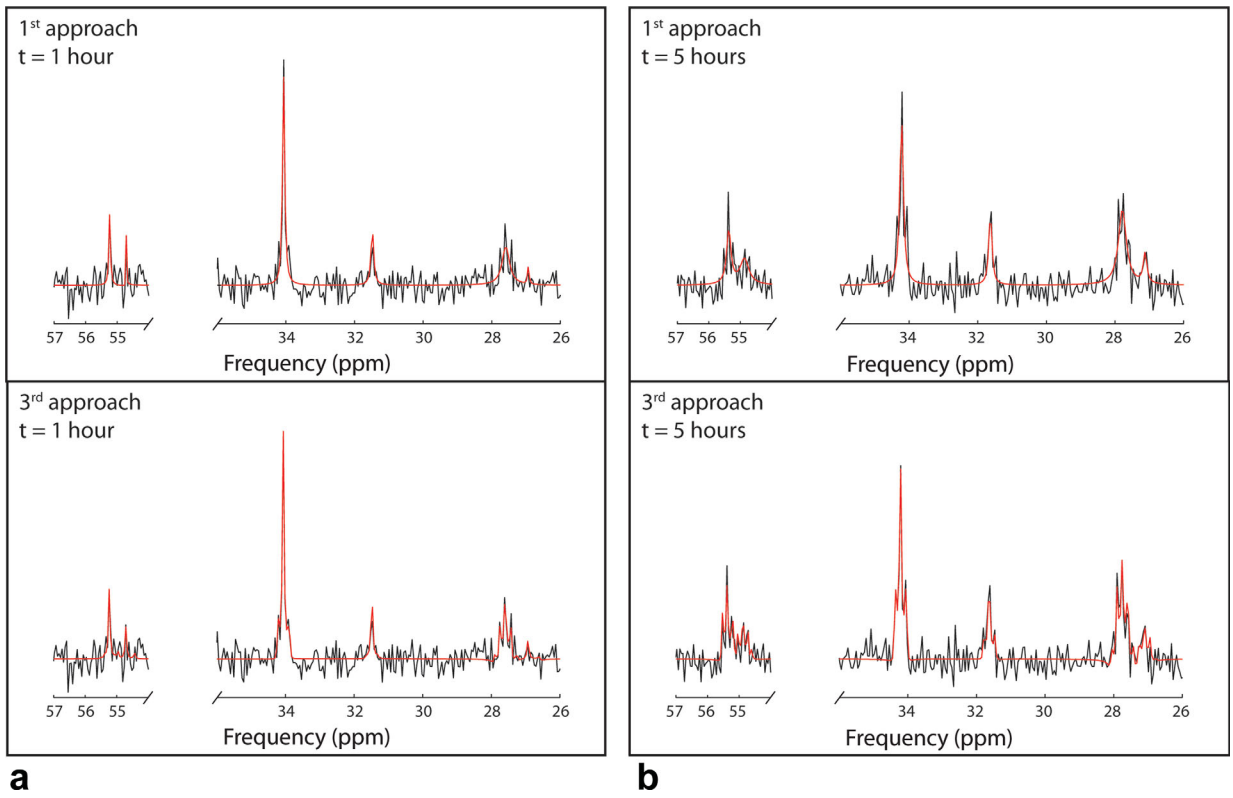


FIG. 5. Quantification of an in vivo $^{13}C$ MRS spectrum acquired with a temporal resolution of 5.4 min (**a**) after 1 h and (**b**) 5 h of infusion. The upper pannel shows the quantification made using the 1st approach (singlet resonances) and the lower panel the quantification using the 3rd approach (multiplet pattern with inclusion of phase distortions). The plotted regions were focused on Glu and Gln C2, C3, and C4 multiplets.

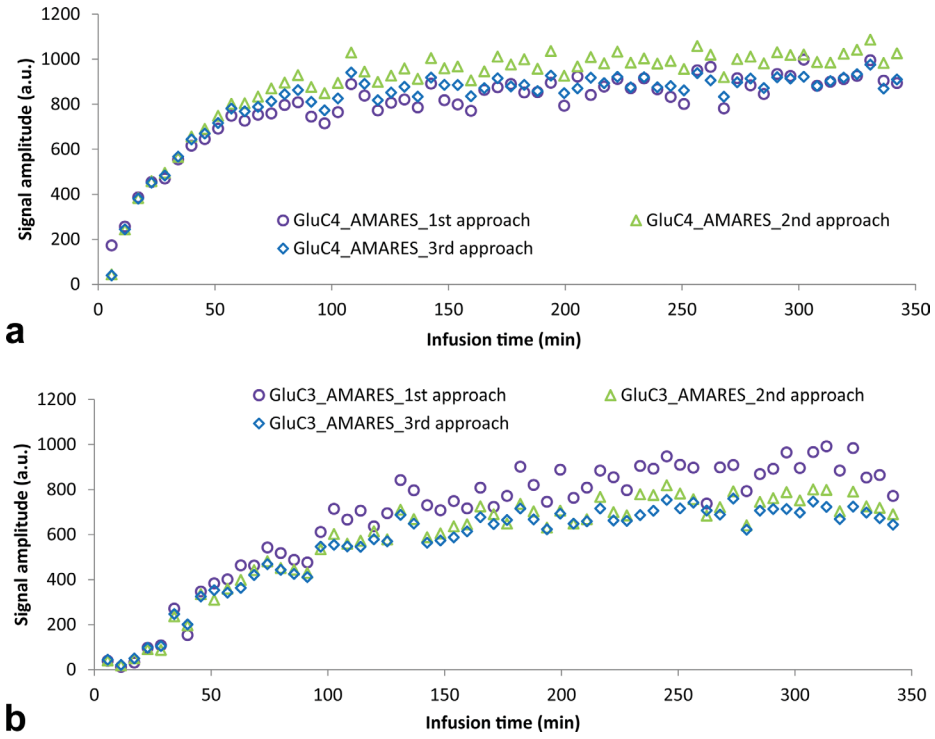


FIG. 6. (**a**) Representative in vivo time courses of GluC4 using AMARES with the 1st (purple circles), 2nd (green triangles) and 3rd (blue rhombus) approach; (**b**) Representative in vivo time courses of GluC3 using AMARES with the 1st (purple circles), 2nd (green triangles) and 3rd (blue rhombus) approach. [Color figure can be viewed in the online issue, which is available at wileyonlinelibrary.com.]

approach), the fit matched satisfactorily the data acquired only in the first hour of infusion. For the spectra acquired later, a substantial mismatch between the original spectra and the fit was observed (Fig. 5b). Figure 6a shows the impact of prior knowledge on the quantification of the GluC4 position whereas Fig. 6b shows the impact of prior knowledge on the labeling position GluC3. As for the Monte Carlo study, when fitting the in vivo data with AMARES combined with low-level prior knowledge (1st approach), large fluctuations of the fitted data were noticed (between 10 and 30%). When the medium-level prior knowledge (2nd approach) was used, slight overestimations ranging from 4 to 13% were obtained.

In a second step we compared the in vivo time courses obtained using AMARES with high-level prior knowledge (3rd approach, blue rhombus and red squares in Fig. 7) with those obtained using LCModel (4th approach, green triangles and orange circles in Fig. 7). As can be seen from the in vivo time courses of Glu C4, C3, C2 and Gln C4, C3, C2, the two approaches gave consistent and highly similar results. Overall, the differences between the two approaches were between 0 and 5%.

## DISCUSSION

This study demonstrates that accurate quantification of in vivo $^{13}$C isotopomers using AMARES combined with a suitable incorporation of high-level prior knowledge is possible. The degree of the prior knowledge necessary for the quantification of in vivo $^{13}$C spectra using AMARES was evaluated first with Monte Carlo simulations using artificial input $^{13}$C MRS spectra and then on in vivo $^{13}$C rat brain spectra. Finally, we compared AMARES and LCModel for the quantification of in vivo rat brain $^{13}$C spectra.

To validate AMARES for the quantification of $^{13}$C isotopomers, we first used Monte Carlo simulations which showed that AMARES combined with high-level prior knowledge (3rd approach) gave consistent and similar results to the true values even at low SNR and large linewidths (Fig. 2b,c). Note that even at a SNR of 1 the obtained systematic errors were below 7% consistent with previous observations (17). Moreover, identical results to those in the Monte Carlo simulations were obtained when AMARES combined with high-level prior knowledge (3rd approach) was used to quantify in vivo $^{13}$C rat brain spectra (Figs. 6 and 7). To evaluate the reliability of in vivo quantifications using the 3rd approach (high-level prior knowledge) we compared our results to those obtained using LCModel, which was previously validated (17) as gold standard. Our data (Fig. 7) showed that the results obtained with AMARES were identical with those obtained with LCModel when high-level prior knowledge was used. This result could be expected since identical prior knowledge was used for both quantification algorithms. The corresponding AMARES prior knowledge files are provided as Supporting Information.

The high sensitivity and spectral resolution with concomitant AMARES quantification combined with high-level prior knowledge indicated that the precision was sufficient to allow the simultaneous measurement and quantification of Glu C4, C3, C2 and Gln C4, C3, C2 with a temporal resolution of 5.4 min in a 320 μL voxel.

To determine the degree of prior knowledge necessary when using AMARES for the quantification of simulated and in vivo $^{13}$C isotopomers measured in rat brain at 9.4T, we compared the results obtained using two different approaches based on low and medium-level prior knowledge to those obtained using high-level prior knowledge. When reducing prior knowledge by fitting

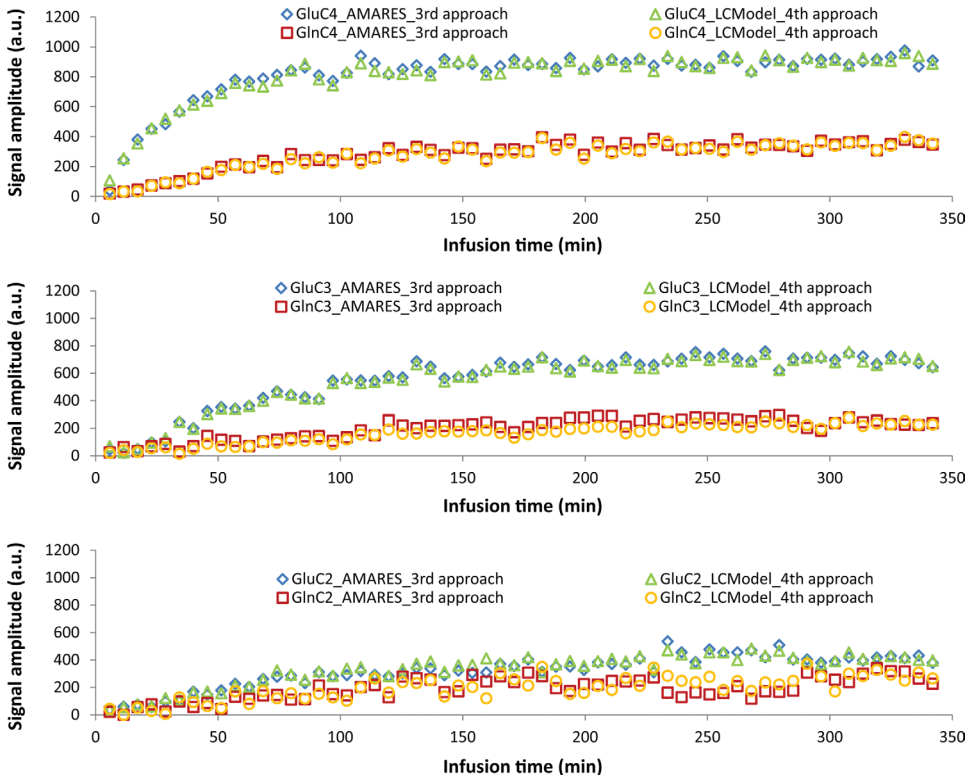


FIG. 7. Representative in vivo time courses of Glu C4, C3, C2 and Gln C4, C3, C2 obtained using AMARES with high-level prior knowledge (3rd approach—blue rhombus and red squares) vs. LCModel (4th approach—green triangles and orange circles). [Color figure can be viewed in the online issue, which is available at wileyonlinelibrary.com.]

each resonance at a specific carbon position with a singlet without taking the J-coupling pattern into account (1st approach) a large fluctuation of the fitted data was obtained combined with an underestimation of GluC4 (~10%) and an overestimation of GluC3 (~30%) for both Monte Carlo and in vivo quantifications (Figs. 2 and 6). The overestimation of GluC3 was attributed to the fitting of a complex multiplet pattern by a singlet with large linewidth.

When further improving the prior knowledge but neglecting the information regarding the relative phase due to homonuclear $^{13}C$-$^{13}C$ *J*-modulation occurring in the DEPT sequence (2nd approach), only slight overestimations ranging from 3 to 13% were obtained for both Monte Carlo and in vivo studies (Figs. 2a and 6). The relative phase due to homonuclear $^{13}C$-$^{13}C$ *J*-modulation occurring in the DEPT sequence was discernable in the spectra through the negative contributions in the isotopomer lines (Fig. 3). When omitting this information in the quantification, an overestimation of the metabolite concentrations was noticed (Figs. 2a, 3b, and 6). Moreover, the relative contribution of the multiplets to each carbon position was biased, potentially leading to errors in the fractional enrichment of the carbon positions, if calculated from the multiplets (when using the 2nd approach).

Overall, the outcome of the Monte Carlo simulations was highly consistent with the in vivo quantification with respect to the importance of high-level prior knowledge, demonstrating that fitting the signals arising from different carbon positions with singlets and neglecting the multiplets due to $^{13}C$-$^{13}C$ J-couplings might lead to substantial errors in the quantification of the time courses which would consequently lead to errors in the estimated metabolic fluxes. These results were independent of the data quality, as demonstrated by our simulations showing that the high-level prior knowledge gave more accurate and reliable results than the 1st approach, even at the lowest SNR values (Fig. 2d,e).

It is interesting to note that the quantification of the time courses for the first hour of infusion was similar for all the AMARES approaches used in this study. However, when the resonances ascribed to the $^{13}C$-$^{13}C$ J-coupling started to have significant intensity, the time courses using the 1st and 2nd approach were no longer consistent, ascribed to the inadequate assumptions on the structure of the resonances. Indeed, upon infusion of [1,6-$^{13}C_2$] glucose, the fractional enrichment of the carbon positions and thus the probability of $^{13}C$ isotopes in adjacent positions increases. Consequently, the splitting of resonances due to homonuclear $^{13}C$-$^{13}C$ scalar coupling is more important. Using the GluC4D43/(GluC4S+GluC4D43) ratio, a glutamate FE of about 20% at the C3 position was estimated after 1 h of [1,6-$^{13}$C2] glucose infusion. Based on our simulations and on the quantification of time courses for the first hour of infusion (corresponding to a FE of ~20%), this value of FE can be considered as an upper threshold for obtaining similar results from both 1st and 3rd approaches. Above this value, the results obtained using the 3rd approach should be more accurate. This observation is also valid for [1-$^{13}C$] glucose infusions, for which this critical FE value is reached at later time points.

We conclude that accurate quantification of in vivo $^{13}C$ isotopomers using AMARES combined with a suitable incorporation of high-level prior knowledge is possible, leading to a more accurate and reliable quantification of in vivo $^{13}C$ spectra and to similar results to those

obtained with LCModel. In contrast, when using limited prior knowledge, the results obtained with AMARES were over/underestimated, demonstrating that fitting the signals arising from different carbon positions with singlets and neglecting the multiplets due to $^{13}C$-$^{13}C$ J-couplings might lead to substantial errors in the quantification of the time courses, which would consequently lead to errors in the estimated metabolic fluxes.

## REFERENCES


1. Henry PG, Adriany G, Deelchand D, Gruetter R, Marjanska M, Oz G, Seaquist ER, Shestov A, Ugurbil K. In vivo 13C NMR spectroscopy and metabolic modeling in the brain: a practical perspective. Magn Reson Imaging 2006;24:527–539.
2. Duarte JMN, Lanz B, Gruetter R. Compartmentalized cerebral metabolism of [1,6–13C]glucose determined by in vivo 13C NMR spectroscopy at 14.1 T. Front Neuroenergetics 2011;3:1–15.
3. van Eijsden P, Behar KL, Mason GF, Braun KP, de Graaf RA. In vivo neurochemical profiling of rat brain by $^{1}H$-[$^{13}C$] NMR spectroscopy: cerebral energetics and glutamatergic/GABAergic neurotransmission. J Neurochem 2010;112:24–33.
4. Gruetter R, Seaquist ER, Ugurbil K. A mathematical model of compartmentalized neurotransmitter metabolism in the human brain. Am J Physiol Endocrinol Metab 2001;281:E100-E112.
5. de Graaf RA, Mason GF, Patel AB, Behar KL, Rothman DL. In vivo $^{1}H$-[$^{13}C$]-NMR spectroscopy of cerebral metabolism. NMR Biomed 2003;16:339–357.
6. Sibson NR, Mason GF, Shen J, Cline GW, Herskovits AZ, Wall JE, Behar KL, Rothman DL, Shulman RG. In vivo $^{13}C$ NMR measurement of neurotransmitter glutamate cycling, anaplerosis and TCA cycle flux in rat brain during. J Neurochem 2001;76:975–989.
7. Gruetter R. In vivo 13C NMR studies of compartmentalized cerebral carbohydrate metabolism. Neurochem Int 2002;41:143–154.
8. Gruetter R. Principles of the measurment of neuro-glial metabolism using in vivo 13C NMR spectroscopy. Adv Mol Cell Biol 2004;31: 409–433.
9. Gruetter R, Adriany G, Choi IY, Henry PG, Lei H, Oz G. Localized in vivo 13C NMR spectroscopy of the brain. NMR Biomed 2003;16: 313–338.
10. Gruetter R, Seaquist ER, Kim S, Ugurbil K. Localized in vivo 13C-NMR of glutamate metabolism in the human brain: initial results at 4 tesla. Dev Neurosci 1998;20:380–388.
11. Uffmann K, Gruetter R. Mathematical modeling of (13)C label incorporation of the TCA cycle: the concept of composite precursor function. J Neurosci Res 2007;85:3304–3317.
12. Choi IY, Lei H, Gruetter R. Effect of deep pentobarbital anesthesia on neurotransmitter metabolism in vivo: on the correlation of total glucose consumption with glutamatergic action. J Cereb Blood Flow Metab 2002;22:1343–1351.
13. Oz G, Berkich DA, Henry PG, Xu Y, LaNoue K, Hutson SM, Gruetter R. Neuroglial metabolism in the awake rat brain: $CO_2$ fixation increases with brain activity. J Neurosci 2004;24:11273–11279.
14. Lebon V, Petersen KF, Cline GW, Shen J, Mason GF, Dufour S, Behar KL, Shulman GI, Rothman DL. Astroglial contribution to brain energy metabolism in humans revealed by $^{13}C$ nuclear magnetic resonance spectroscopy: elucidation of the dominant pathway for neurotransmitter glutamate repletion and measurement of astrocytic oxidative metabolism. J Neurosci 2002;22:1523–1531.
15. Deelchand DK, Nelson C, Shestov AA, Ugurbil K, Henry PG. Simultaneous measurement of neuronal and glial metabolism in rat brain in vivo using co-infusion of [1,6-$^{13}C_2$]glucose and [1,2-$^{13}C_2$]acetate. J Magn Reson 2009;196:157–163.
16. Henry PG, Tkac I, Gruetter R. 1H-localized broadband 13C NMR spectroscopy of the rat brain in vivo at 9.4 T. Magn Reson Med 2003; 50:684–692.
17. Henry PG, Oz G, Provencher S, Gruetter R. Toward dynamic isotopomer analysis in the rat brain in vivo: automatic quantitation of 13C NMR spectra using LCModel. NMR Biomed 2003;16:400–412.
18. Vanhamme L, Van Huffel S, Van Hecke P, van Ormondt D. Time-domain quantification of series of biomedical magnetic resonance spectroscopy signals. J Magn Reson 1999;140:120–130.
19. Gruetter R. Automatic, localized in vivo adjustment of all first- and second-order shim coils. Magn Reson Med 1993;29:804–811.
20. Gruetter R, Tkac I. Field mapping without reference scan using asymmetric echo-planar techniques. Magn Reson Med 2000;43:319–323.
21. Mlynarik V, Gambarota G, Frenkel H, Gruetter R. Localized short-echo-time proton MR spectroscopy with full signal-intensity acquisition. Magn Reson Med 2006;56:965–970.
22. Silver MS, Joseph RI, Chen CN, Sank VJ, Hoult DI. Selective population inversion in NMR. Nature 1984;310:681–683.
23. Tkac I, Starcuk Z, Choi IY, Gruetter R. In vivo 1H NMR spectroscopy of rat brain at 1 ms echo time. Magn Reson Med 1999;41:649–656.
24. Provencher SW. Estimation of metabolite concentrations from localized in vivo proton NMR spectra. Magn Reson Med 1993;30:672–679.
25. Provencher SW. Automatic quantitation of localized in vivo 1H spectra with LCModel. NMR Biomed 2001;14:260–264.
26. Jeffrey FM, Storey CJ, Sherry AD, Malloy CR. 13C isotopomer model for estimation of anaplerotic substrate oxidation via acetyl-CoA. Am J Physiol 1996;271(4 Part 1):E788-E799.
27. Hertz L, Dienel GA. Energy metabolism in the brain. Int Rev Neurobiol 2002;51:1–102.
28. Badar-Goffer RS, Bachelard HS, Morris PG. Cerebral metabolism of acetate and glucose studied by 13C-NMR spectroscopy. A technique for investigating metabolic compartmentation in the brain. Biochem J 1990;266:133–139.
29. Ebert D, Haller RG, Walton ME. Energy contribution of octanoate to intact rat brain metabolism measured by 13C nuclear magnetic resonance spectroscopy. J Neurosci 2003;23:5928–5935.
30. Berliner LJ, Robitaille PM. In vivo carbon-13 NMR. New York: Kluwer; 1998.